



Mapping the forest disturbance regimes of Europe

Cornelius Senf^{1,2}✉ and Rupert Seidl^{1,2,3}

Changes in forest disturbances can have strong impacts on forests, yet we lack consistent data on Europe's forest disturbance regimes and their changes over time. Here we used satellite data to map three decades of forest disturbances across continental Europe, and analysed the patterns and trends in disturbance size, frequency and severity. Between 1986 and 2016, 17% of Europe's forest area was disturbed by anthropogenic and/or natural causes. We identified 36 million individual disturbance patches with a mean patch size of 1.09 ha, which equals an annual average of 0.52 disturbance patches per km² of forest area. The majority of disturbances were stand replacing. While trends in disturbance size were highly variable, disturbance frequency consistently increased and disturbance severity decreased. Here we present a continental-scale characterization of Europe's forest disturbance regimes and their changes over time, providing spatial information that is critical for understanding the ongoing changes in Europe's forests.

Forests cover 33% of Europe's total land area and provide important ecosystem services to society, ranging from carbon sequestration to the filtration of water, and protection of soil from erosion and human infrastructure from natural hazards¹. Europe's forests have expanded in recent decades² and have accumulated substantial amounts of biomass due to intensive post-World War II reforestation programmes, changes in management systems and timber-harvesting rates that have remained below increment³. This success story of twentieth-century forestry in Europe, however, also has side effects, because the resultant changes in forest structure and composition have—in combination with climate change—led to an episode of increasing forest disturbances in recent decades^{4–7}. Increasing forest disturbances have the potential to erode Europe's carbon storage potential^{8,9} and also impact other important ecosystem services provided by Europe's forests^{10,11}. Given the predicted increase in demand for wood¹ and an expected future intensification of forest dieback under climate change¹², it is fundamental to both understand and increase the resilience of Europe's forests to changing disturbances^{13–15}.

Understanding the ongoing changes in forest ecosystems and developing management strategies to increase their resilience require a robust quantitative understanding of the prevailing disturbance regimes^{16,17}. Disturbance regimes characterize the cumulative effects of all disturbance events occurring in a given area and time period, and are often characterized by metrics such as the size, frequency and severity of disturbances occurring in a given area¹⁶. In Europe, forests have been utilized by humans for centuries, transforming species composition and structure^{18–20} and, consequently, also the natural disturbance regimes of forests. In addition to this indirect effect, human land use is directly disturbing forest canopies through timber harvesting, altering the rate and spatial patterns of forest disturbances compared to natural systems²¹. Human land use also interacts with natural disturbances—for example, by salvage logging of disturbed timber²² and shortening early seral stages through planting²³. More broadly, forest management alters biological legacies and landscape structure^{23,24}, with feedbacks on subsequent disturbances. Due to the intricate linkages between natural and human processes driving forest disturbances in Europe, characterization of the disturbance regimes of Europe's forests requires a holistic perspective covering both natural and human disturbances.

In regard to Europe there is currently little quantitative information available on disturbance regimes and their changes over time, especially when considering both natural and human disturbances. While previous studies have characterized the disturbance regimes of some of Europe's forest ecosystems^{4,18,25–27}, those studies have either focused on purely natural processes, lack a spatially and temporally consistent data source or focus only on the regional scale. Due to this lack of quantitative information at a continental scale, we do not know, for instance, how disturbance size, frequency and severity vary across Europe. Furthermore, while recent studies indicate an increase in disturbance rates across Europe's natural and managed forests^{4,6}, it remains unknown whether this change is mainly the result of changes in disturbance frequency (that is, more disturbance events) or disturbance size (that is, larger individual disturbance patches). Likewise, our quantitative knowledge of changes in disturbance severity is scant and it remains unclear whether disturbances in Europe have become more severe in recent decades (for example, through increased burn severity²⁸) or whether recent changes in forest management approaches (for example, the adoption of 'close-to-nature' silviculture²⁹) have reduced disturbance severity as reported for parts of central Europe⁴, for instance.

Here, our aim was to map and characterize the disturbance regimes of Europe's forests for the period 1986–2016. Our specific research questions were: (1) what are the size, frequency and severity of forest disturbances across Europe's forests? (2) How have the size, frequency and severity of forest disturbances changed over the past three decades? We addressed these two questions by mapping forest disturbance occurrence and severity continuously for continental Europe (35 countries covering 210 million ha of forest) at a spatial grain of 30 m, using >30,000 satellite images and nearly 20,000 manually interpreted reference plots. Subsequently we characterized both the spatial variation in disturbance size, frequency and severity and their temporal trends over time at the continental scale, thus providing the quantitative baseline critically needed for understanding current changes in Europe's forest ecosystems.

Results

In the following sections we present disturbance maps and regimes and, finally, the trends in disturbance regimes in separate sections.

¹Ecosystem Dynamics and Forest Management Group, Technical University of Munich, Freising, Germany. ²Institute for Silviculture, University of Natural Resources and Life Sciences (BOKU), Vienna, Austria. ³Berchtesgaden National Park, Berchtesgaden, Germany. ✉e-mail: Cornelius.senf@tum.de

Disturbance maps. We identified a total of 36 million individual disturbance patches occurring across Europe in the period 1986–2016, equalling a disturbed forest area of 39 million ha or 17% of Europe's forest area (Fig. 1). The overall accuracy of the map was $87.6 \pm 0.5\%$ (mean \pm s.e.m.), with a commission error of $17.1 \pm 1.6\%$ and an omission error of $36.9 \pm 0.02\%$ for detection of disturbances (see Supplementary Table 2). Omission errors were mainly related to low-severity disturbances that could not be separated from noise (Extended Data Fig. 1). The mean absolute error between the estimated disturbance year and manually interpreted disturbance year was 3 years (Extended Data Fig. 2), with 77% of the assigned disturbance years being within 3 years of the manually interpreted disturbance year. We derived a continuous value ranging from zero to one as a measure of disturbance severity (see Fig. 1c). The severity measure expresses the probability of a disturbance being stand replacing, with zero indicating no change in the dominant canopy and one indicating a complete removal of the forest canopy in a disturbance. The disturbance severity measure was well able to differentiate between undisturbed areas (no loss of forest canopy), non-stand-replacing disturbances (partial loss of forest canopy) and stand-replacing disturbances (complete loss of forest canopy; Extended Data Fig. 3), and thus well represents the variable disturbance severity prevailing across Europe's forests.

Disturbance regimes. The average patch size of forest disturbances was 1.09 ha, but disturbance size distribution was highly left-skewed (Fig. 2b). The median disturbance size was only 0.45 ha, with 78% of disturbances <1 ha and 99% <10 ha (Table 1). The largest annual disturbance patch mapped across Europe was a 16,617-ha large forest fire that occurred in 2012 in southern Spain. The average annual disturbance frequency was 0.52 patches per km² of forest area (median, 0.37 patches per km²), with the highest frequencies (highest 1%) ranging from 3 to 31 patches per km² (Table 1). Disturbance severity ranged from 0.22 to 1.00, with an average of 0.77 (median, 0.83). In other words, more than half of disturbed patches across Europe had a very high probability of being stand replacing, indicating a high prevalence of high-severity disturbances.

Spatial variability in the size, frequency and severity of forest disturbances is high across Europe (Fig. 2). Disturbance patches are generally larger in northern and southern Europe compared to central Europe. Also, eastern Europe has larger disturbance patches compared to western Europe (Fig. 2). Above-average disturbance frequencies were found in parts of central Europe, the hemi-boreal zone, parts of France and the Iberian Peninsula (Fig. 2). The highest disturbance frequencies (that is, >3 patches per km²) occurred almost exclusively in Portugal. Disturbance severity was more evenly distributed than the other two disturbance regime indicators (Fig. 2), with a tendency towards higher severities in the Atlantic forests of Ireland and the United Kingdom, the Iberian Peninsula, the Po Valley in Italy and the Pannonic Basin. In contrast, low disturbance severities were recorded for south-eastern Europe along the Dinaric mountain range, as well as in the Apennine mountains of Italy.

Trends in disturbance regimes. Disturbance regimes changed profoundly between 1986 and 2016, but trends differed according to disturbance regime indicator (Fig. 3). Changes in disturbance size were variable across Europe. Hot spots of increasing disturbance size were observed in the Baltic states, the United Kingdom, Ireland and Italy (Fig. 3), whereas trends were largely negative in eastern Germany, western Poland and south-eastern Europe (Fig. 3). Disturbance frequency showed a more consistent increase than disturbance size, with the former increasing in 74% of Europe's forest area (Table 2). Hot spots of increasing disturbance frequency were located in central and eastern Europe (Fig. 3), whereas negative trends were found for Belarus, Albania and Greece as well as parts

of western Europe and northern Fennoscandia (Fig. 3). In contrast, disturbance severity decreased in 88% of the European forest area (Table 2) with particularly strong negative trends in central and south-eastern Europe (Fig. 3).

While mean disturbance size generally increased across Europe (65% of Europe's forests showed an increasing trend in mean disturbance size; Table 2), median disturbance size was more stable (increasing for only 19% of Europe's forests; Table 2). Hence, disturbance size distribution widened over time with an increase in large disturbance patches (that is, in the 75% quantile and maximum disturbance patch size distribution; Table 2) in approximately half of Europe's forests. Overall, changes in disturbance frequency explained 71% of the variability in changing disturbance rates (that is, the trend for the annual percentage of forest area disturbed), whereas changes in disturbance size accounted for only 24% (Extended Data Fig. 4). Thus, the changes in forest disturbance rates observed in Europe are primarily driven by more frequent disturbances and only to a lesser extent by increasing disturbance size.

Discussion

Here we provide a quantitative and spatially explicit characterization of Europe's forest disturbance regimes, highlighting the wide variety in disturbance size, frequency and severity prevailing across the European continent. While forest type and general biophysical environment certainly explain part of the variability in disturbance regimes across Europe^{6,30}, it is probably also the variability in forest management approaches across Europe's forests that plays a fundamental role in explaining the observed patterns. Forest management approaches across Europe range from the small-scale, aiming for continuous forest cover, to even-aged forestry based on clear-felling and high-intensity, short-rotation systems^{31,32}. Many countries that predominantly use small-scale management approaches (for example, Slovenia and Switzerland³³) were characterized by substantially smaller disturbance size and lower disturbance severity in our data (Extended Data Fig. 5), despite also experiencing large-scale natural disturbances³⁴. This clearly contrasts with countries that largely apply even-aged forest management approaches (for example, Finland and Sweden³⁵) or have high proportions of plantation forests (for example, Denmark, Hungary and Ireland¹) which have, on average, larger patch sizes and higher disturbance severity (Extended Data Fig. 5). Disturbance regimes thus varied widely among countries, reflecting differences in management objectives and management histories³⁶. In some instances, these differences occur even for countries that have very similar forest types and biophysical environments, which would suggest a comparable natural disturbance regime (see, for example, Extended Data Fig. 6 for additional examples). A substantial part of the spatial variability in disturbance size, frequency and severity observed here is thus probably driven by variation in forest management across the European continent.

The disturbance regimes of Europe's forests are changing profoundly. Here we show that the previously reported increase in disturbance rates^{4,7} is primarily an effect of increasing disturbance frequency, while disturbance patch size distributions are becoming more variable and disturbance severities are decreasing. The strong increase in disturbance frequencies may be caused by an increase in both wood production and natural disturbances reported throughout Europe⁹, with both factors probably interacting (that is, increasing natural disturbances triggering increased salvage harvesting). The widening of patch size distribution probably results from the combined effects of changes in management approaches towards smaller intervention sizes (that is, single-tree or group selection²⁹) and simultaneous increase in natural disturbance activity, leading to infrequent but large canopy removals (for example, large-scale storm events³⁷ or large-scale fires³⁸). Moreover, multiple disturbance agents, such as bark beetle and wind-throw, or bark beetle

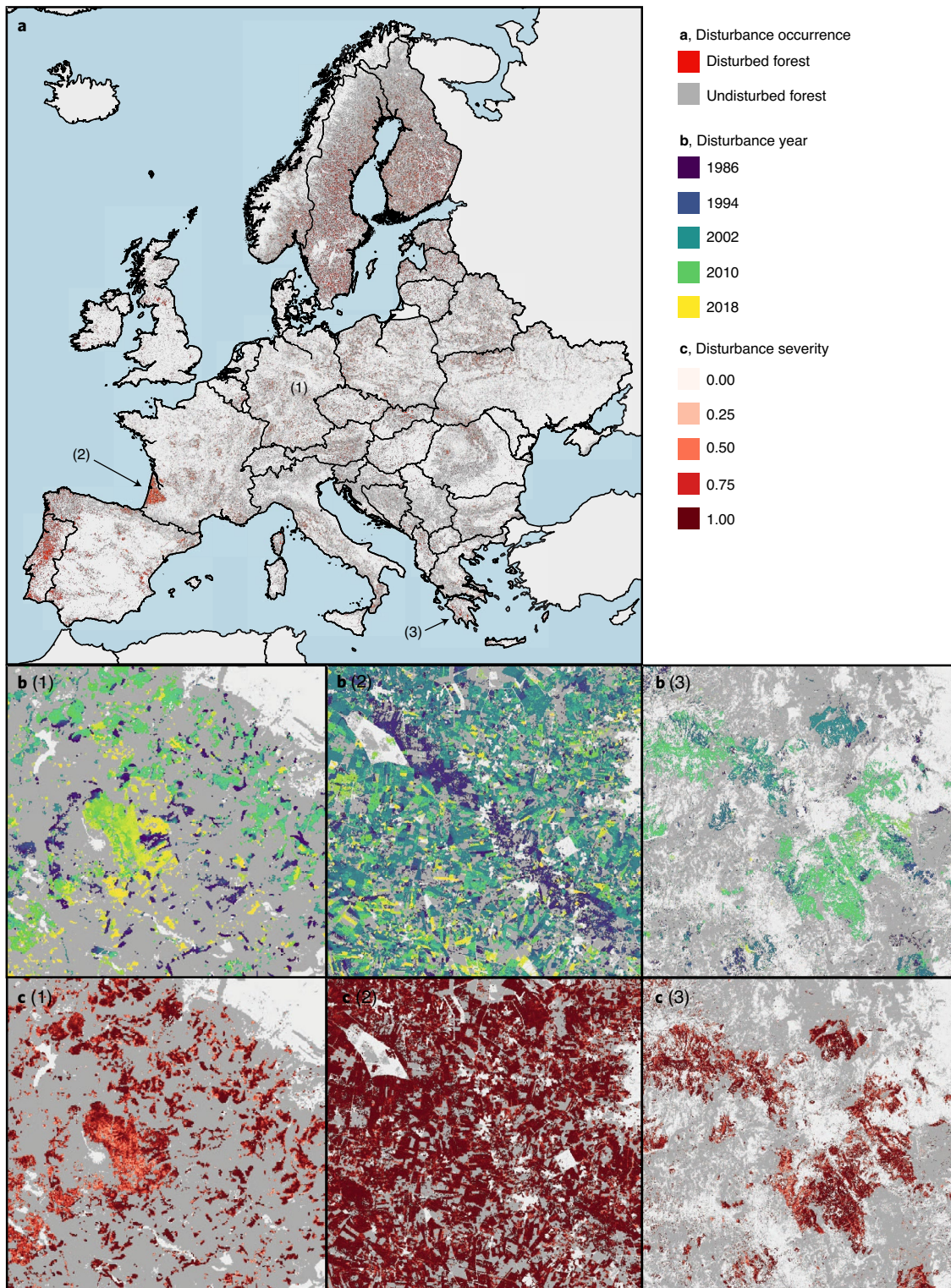


Fig. 1 | Forest disturbances in Europe, 1986–2016. **a**, The occurrence of disturbances across Europe. **b**, Year of disturbance. **c**, Severity of disturbance for three selected areas (scale, 0–1): (1) a bark beetle outbreak of varying severity in and around the Harz National Park (Germany); (2) salvage-logged wind disturbance in an intensively managed plantation forest in the Landes de Gascons (France), with very high disturbance severity; and (3) fire disturbances on the Peloponnese peninsula (Greece), with variable burn severity. Disturbance maps were derived from analysis of >30,000 Landsat images across continental Europe. See Extended Data Fig. 7 for a high-quality version of the main disturbance map.

and subsequent salvage logging, can lead to aggregation of several smaller disturbance patches into one large disturbance patch if the intact forest matrix between patches is removed. That is, while individual patches might be small, multiple interacting disturbance

agents can lead to the agglomeration of several smaller patches into one larger patch over time. The combined effects of changes in management approaches and natural disturbances also probably explain continental-scale decreases in disturbance severity, because

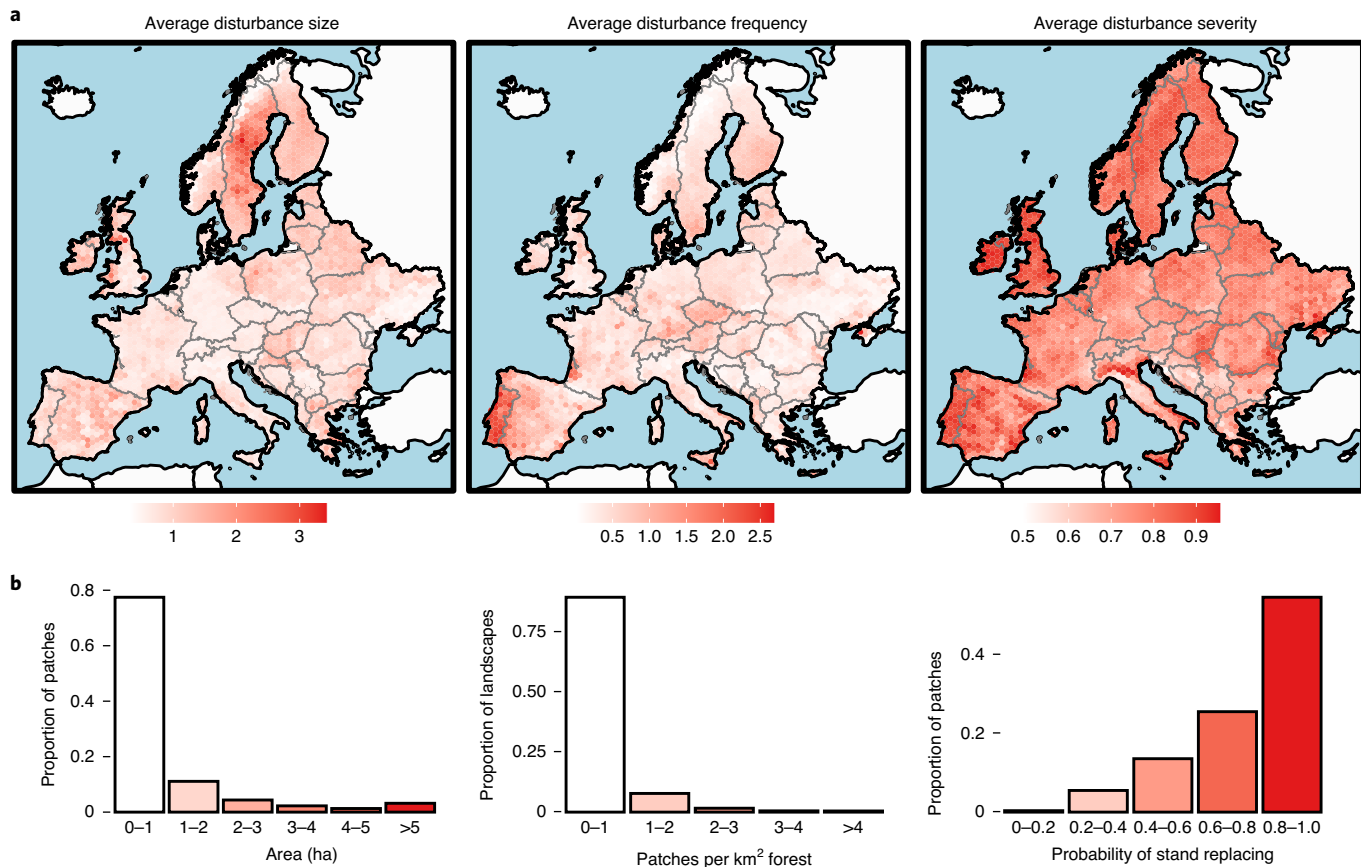


Fig. 2 | Forest disturbance regimes mapped across Europe. **a**, Maps of average disturbance size (ha), frequency (patches per km² forest area) and severity (scale, 0–1) calculated for hexagons on a 50-km grid across continental Europe. Background maps are derived from <https://gadm.org>. **b**, Distribution of average disturbance size, frequency and severity across Europe.

Table 1 | Distribution of the size, frequency and severity of disturbances across Europe's forests

Indicator	Description	Mean	Quantiles (%)						
			0	1	25	50	75	99	100
Size	Size of disturbed patch (ha)	1.09	0.18	0.18	0.27	0.45	0.90	10.10	16,617.42
Frequency	Disturbance patches per km ² forest	0.52	<0.01	0.02	0.20	0.37	0.63	3.01	31.21
Severity	Probability of a disturbed patch being stand replacing (that is, complete loss of forest canopy)	0.77	<0.01	0.22	0.65	0.83	0.94	1.00	1.00

See Supplementary Table 3 for values by country.

management systems are increasingly optimized to reduce impact³⁹ and many natural disturbances that occur frequently (that is, bark beetle infestations and small-scale wind-throw) are characterized by mixed severity⁴⁰.

Here we provide a high-resolution forest disturbance map for continental Europe covering three decades of forest development, a dataset of importance for future research on the dynamics of Europe's forests. Nevertheless, there are methodological limitations that should be considered when using the data presented here. First, we do not distinguish disturbance agents in our analysis—currently an individual disturbance patch cannot be attributed specifically to either natural or human origin. While recent methodological advances have been made in attributing disturbance agents, founded on satellite-based forest change products⁴¹, those approaches are not yet applicable at the spatial and temporal scale of our analysis. The

key reasons for this are (1) missing reference data on the actual occurrence of disturbance agents and (2) the fact that management signals are often superimposed on natural disturbances (that is, subsequent salvage logging). Future work should thus aim for improved attribution algorithms that consider more explicitly the complex interactions between human and natural processes in Europe's forest ecosystems. Second, in this paper we map only the greatest disturbance per pixel—that is, there is only one disturbance event recorded for the whole 30-year period for each 30 × 30-m² pixel. For short-rotation systems we thus might miss some disturbances if, for example, two harvests have occurred in the past three decades. Finally we note that, despite careful processing, satellite data can be noisy, preventing the detection of very-low-severity disturbances. This limitation is intrinsic to the data used herein but there are, however, very few alternative data sources that allow the consistent analysis of forest dynamics

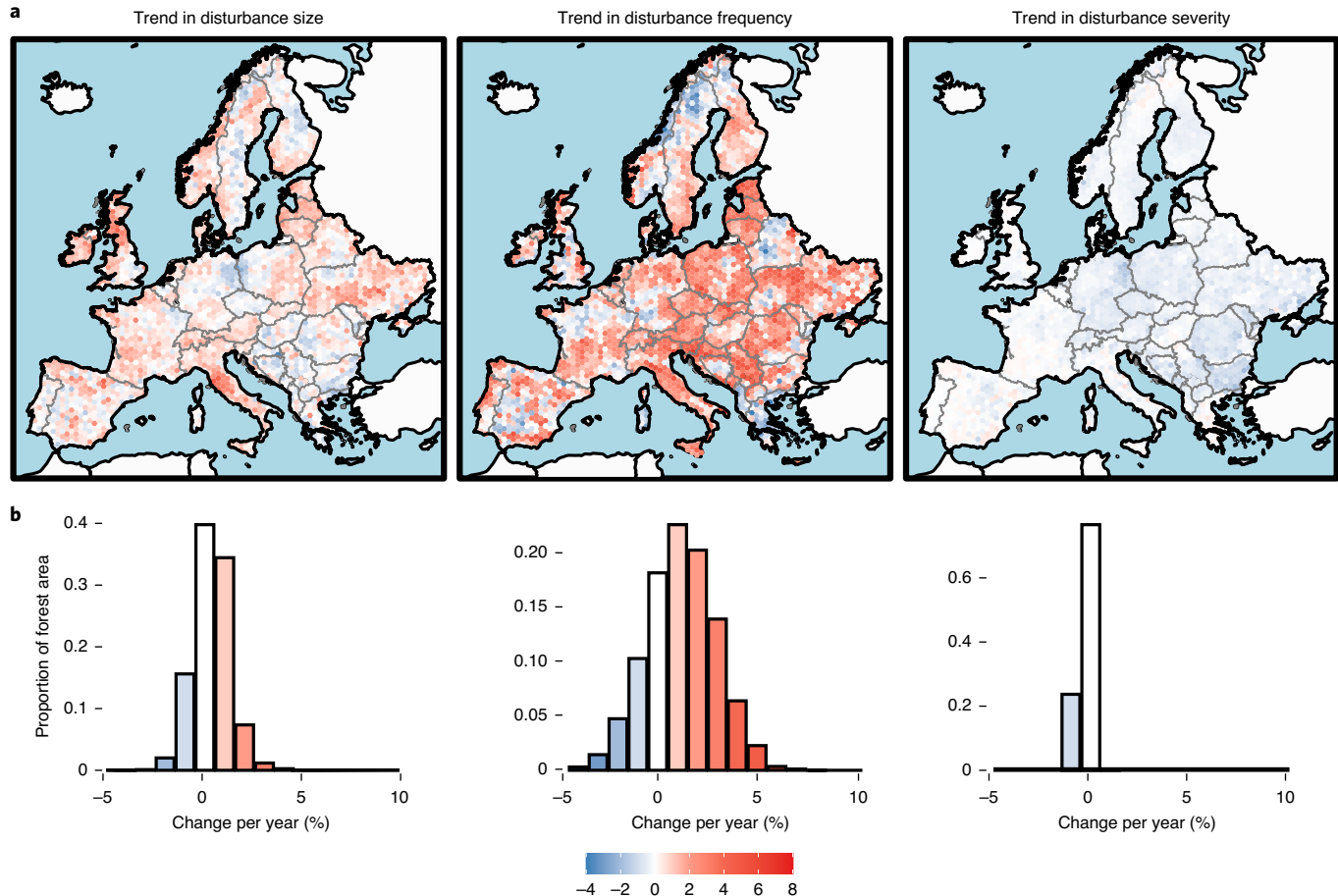


Fig. 3 | Trends in Europe's forest disturbance regimes, 1986–2016. **a**, Maps of trends in disturbance size, frequency and severity calculated as a 50-km hexagon grid across continental Europe. Background maps are derived from <https://gadm.org>. **b**, Distribution of forest area among trend classes.

Table 2 | Distribution of the trends in size, frequency and severity of disturbances across Europe's forests, 1986–2016

Indicator	Mean (across disturbed patches)	Mean (weighted by forest area)	Proportion of forest area with positive trends	Proportion of forest area with no trend
Size (ha)				
Mean	0.41	0.33	0.65	0.00
50% quantile	0.21	0.23	0.19	0.78
75% quantile	0.53	0.53	0.54	0.32
100% quantile	0.35	0.15	0.52	0.00
Frequency (no. per km ² forest area)	1.17	1.19	0.74	0.01
Severity (0–1)				
Mean	-0.31	-0.33	0.12	0.00

See Supplementary Table 3 for values by country.

Methods

In the following we describe the reference data, disturbance mapping algorithm and characterization of disturbance regimes using spatial pattern analysis.

Reference data. The acquisition of consistent reference data across large areas—such as continental Europe—is challenging. In this study we made use of manually interpreted satellite data, which served as a valuable alternative to field-based data⁴⁵. Manual interpretation of satellite data for calibration and validation of Landsat-based forest change maps is a well-established approach and has previously been used in numerous studies^{43–46}. In essence, an interpreter inspects the temporal profile of the spectral trajectory of a Landsat pixel and, with the help of Landsat image chips and the very-high-resolution imagery available in Google Earth, makes a well-informed call as to whether the trajectory represents stable forest canopy cover or a mortality event occurred⁴⁷. Here we used a previously established set of 19,996 interpreted Landsat pixels⁷ as reference data. The initial sample was drawn at random from European forests, with samples stratified by country (500 samples per country). Because interpreters might declare a plot as no-forest during interpretation (resulting from errors in the automatically generated forest mask used as the basis for stratified sampling), the realized sample size varied among countries (Supplementary Table 1). The response design followed well-documented protocols developed and published previously⁴⁷. Manual interpretation was performed by a total of nine interpreters using established software tools⁴⁷, and the data are freely accessible under the following repository: <https://doi.org/10.5281/zenodo.3561925>.

The reference sample set consisted only of forest pixels, and there was thus a need to substitute the sample with non-forest reference pixels. We therefore drew a country-stratified sample of non-forest pixels using a Landsat-based land-cover map from ref. ⁴⁸. Each country's sample size was chosen to match the forest proportion of that country (based on data from the FAOSTATS database)—that is, the total sample of each country equalled a random sample across its terrestrial forested and non-forested land surface areas (see Supplementary Table 1). In total we drew 46,461 non-forest reference pixels that, paired with the 19,996 forest reference pixels manually interpreted, totalled 66,457 reference pixels available for

over three decades at the continental scale. Despite these limitations, we are confident that our quantitative and spatially explicit analysis of patterns and trends in forest disturbances provides a crucial step towards better understanding of the ongoing changes in Europe's forest ecosystems.

calibration and validation. From the full reference sample we randomly drew a subsample of 5,000 pixels for map validation, with the remaining 61,457 pixels used for model calibration. The validation subsample was drawn in proportion to the size of each country, to ensure a consistent and unbiased estimation of mapping accuracies for the final European map product.

Mapping disturbances. At the core of our mapping workflow we rely on an established time-series segmentation approach called LandTrendr⁴⁹, implemented in the high-performance, cloud-computing environment Google Earth Engine⁵⁰. In essence, LandTrendr segments annual Landsat pixel time series into linear features for which a set of metrics can be extracted. Here we do not provide details on the underlying LandTrendr routines but focus instead on the salient details of our mapping workflow (see Supplementary Fig. 1 for a graphical outline). The workflow was based on code published in Kennedy et al.⁵⁰.

In a first step we screened all available Tier 1 Landsat 4, 5, 7 and 8 images in the United States Geological Survey archive. Tier 1 images are delivered as ready-to-use surface reflectance images including a cloud mask, but we used coefficients from Roy et al.⁵¹ to spectrally align the varying sensor types used on board Landsat 4/5 (Thematic Mapper), Landsat 7 (Enhanced Thematic Mapper Plus) and Landsat 8 (Operational Land Imager). After spectral alignment we filtered all available images for summer-season acquisition dates (1 June to 30 September) and built annual medoid composites following Flood⁵².

Second, we ran LandTrendr for two spectral bands (shortwave infrared I and II) and two spectral indices commonly used for forest disturbance and mortality mapping^{45,46,53–55}: tasselled cap wetness and normalized burn ratio. We used a standard parameter set for LandTrendr with no filtering or thresholding, thus allowing for maximum sensitivity in detection of change (that is, allowing for high commission error).

Third, we extracted the greatest change segment from each pixel's LandTrendr trajectory, fit to both spectral bands and both spectral indices. From this segment we derived a set of three metrics describing the magnitude, duration and rate of change⁵³, as well as a measure of the signal-to-noise ratio as described in Cohen et al.⁵⁴. We further derived the spectral band/index value before, and the rate of change following, the greatest change segment. Metrics similar to those used here have also been applied in previous studies mapping forest cover changes^{44,46,55}.

Fourth, we used the set of metrics derived from the greatest change segment for the two spectral bands and the two spectral indices, the calibration data outlined in the previous section and random forest classification⁵⁶ to classify each pixel into either no-forest, undisturbed forest or disturbed forest (that is, at least one disturbance event during the study period). This last step filters out commission errors introduced by LandTrendr and thus greatly improves mapping accuracy compared to purely automatic algorithms⁵⁷. Nevertheless, we experienced difficulties in correctly separating forest and no-forest areas based solely on LandTrendr outputs. This was due to high spectral changes in agricultural areas that were identified as disturbances by LandTrendr. To tackle this problem, we added a 3-yr tasselled cap brightness, greenness and wetness median composite centred on 1985 and 2018, respectively, to the classification stack. The additional six bands delivered more detailed spectral information on stable forest and non-forest pixels. Finally, we applied the trained random forest model to the full classification stack (that is, LandTrendr metrics from the two spectral bands and two spectral indices plus the tasselled cap composite from 1985 and 2018) to consistently map the categories no-forest, undisturbed forest and disturbed forest across continental Europe. We validated the final map using the validation subsample described in the previous section. We derived a confusion matrix and report overall accuracy, errors of commission and errors of omission following best-practice recommendations given in ref. ⁴².

Fifth, while the map thus derived indicates whether a mortality event has happened, it does not provide information on when that event happened. We therefore calculated the year of disturbance onset (that is, the year of greatest spectral change) from all spectral bands and spectral indices using an automated majority vote. If there was a tie (for example, all four bands/indices indicated a different year), we reverted to the median value. To validate this processing step, we compared the year assigned from LandTrendr to the manually interpreted year of disturbance for the 5,000 reference plots.

Spatial filtering. The last step in creating disturbance maps for continental Europe was to apply a set of spatial filters for removal of unrealistic outliers from the resulting disturbance maps and enhancement of spatial pattern analysis. We first set a minimum mapping unit of two $30 \times 30\text{-m}^2$ pixels (that is, 0.18 ha) and removed all disturbance patches smaller than the minimum mapping unit. In a second filtering step, we identified all patches smaller than the minimum mapping unit for each year and assigned these to the year of the surrounding disturbed pixels (if any), thus accounting for artefacts related to uncertainties in the correct identification of the disturbance year (see Supplementary Fig. 2). In a final filtering step, we removed holes within disturbance patches smaller than the minimum mapping unit by filling them with the year of the surrounding pixels. While the filtering was done to improve the spatial analyses described in the following section, we note that it was applied after accuracy assessment. That assessment thus reports the raw classification performance with no additional filtering.

Characterization of disturbance regimes and their changes. From the annual forest disturbance maps we calculated three disturbance regime indicators based on Turner¹⁶ and Johnstone et al.¹⁷: disturbance size, frequency and severity. Disturbance size and severity were calculated at the patch level and were subsequently aggregated to the landscape level, while disturbance frequency was calculated directly at the landscape level. Disturbance size is the number of disturbed pixels for each individual patch (patches were defined annually using rook-contiguity) multiplied by pixel size (0.09 ha). For calculation of disturbance frequency, we subdivided the total study area into a $50 \times 50\text{-km}^2$ hexagon grid (here representing the landscape scale, hexagon area of $2,165\text{ km}^2$), with a total number of 3,240 hexagons across Europe's land area. We chose hexagons over squares because the former minimize spatial differences to the more complex landforms of the European continent and the borders of European countries⁵⁸. For each hexagon, we counted the number of individual disturbance patches per year and divided this by the total forest area within the hexagon, resulting in a measure of the number of disturbed patches per km^2 forest area per year as an indicator of disturbance frequency.

For quantification of disturbance severity we made use of spectral change magnitude provided by the LandTrendr analysis. Spectral change magnitude is well correlated with changes in forest structure during disturbance^{45,53,59}, and here we use it as proxy for disturbance severity. To combine and scale the spectral change magnitude from all four spectral bands/indices into one measure of disturbance severity, we used logistic regression to predict the occurrence of stand-replacing disturbances from the four spectral change magnitudes. Data on stand-replacing disturbances were generated from the reference sample by analysis of manually interpreted land cover after a disturbance segment. If the land cover switched to non-treed following a disturbance segment (for example, after clear-cut harvest or high-intensity fire), the disturbance was assumed to be stand replacing. If the land cover remained treed following a disturbance segment (for example, following a thinning operation or a low-intensity wind-throw), the disturbance was classified as non-stand replacing. This method is based on Senf et al.⁴, who showed that visual interpretation of post-disturbance land cover is an accurate measure for separation of stand-replacing from non-stand-replacing disturbances. By predicting the occurrence of stand-replacing disturbances (that is, complete removal of the canopy and thus a disturbance of very high severity) we scale spectral change magnitude to a value between zero and one, where one indicates complete loss of the canopy (that is, high-severity disturbance) and values close to zero indicate little change in the forest canopy (that is, low-severity disturbance). Intermediate values represent variable levels of canopy loss and thus intermediate disturbance severity. While it is difficult to validate this proxy retrospectively across Europe (that is, no reliable pan-European data are available for canopy changes during past disturbance events), we performed indirect validation by comparing the disturbance severity measure among stand-replacing disturbances, non-stand-replacing disturbances and undisturbed reference pixels.

For spatial visualization of disturbance size, frequency and severity, as well as for calculation and visualization of trends, we aggregated patch-based metrics (that is, disturbance size and severity) to the landscape level (that is, the hexagon) by calculating the arithmetic mean. We report the mean over the median because the former is sensitive to changes in both the central tendency and spread of distribution, but we also include other descriptors in the tables and Supplementary information. Trends in disturbance size, frequency and severity were quantified using a non-parametric Theil-Sen estimator, which is a non-parametric measure of monotonic trends in time series insensitive to outliers⁶⁰.

Reporting Summary. Further information on research design is available in the Nature Research Reporting Summary linked to this article.

Data availability

The Landsat data are freely available via either USGS Earth Explorer (<https://earthexplorer.usgs.gov>) or Google Earth Engine (<https://earthengine.google.com>). The reference data used in this paper are available at <https://doi.org/10.5281/zenodo.3561925>. All other data used are available at <https://doi.org/10.5281/zenodo.3925447>. The disturbance maps produced in this paper are available at <https://doi.org/10.5281/zenodo.3924381>.

Code availability

The code used for processing the Landsat data is available at <https://github.com/eMapR/IT-GEE>. The code for reproduction of all analyses is available at <https://doi.org/10.5281/zenodo.3925447>.

Received: 20 January 2020; Accepted: 17 August 2020;
Published online: 14 September 2020

References

1. State of Europe's Forests 2015 Report (Forest Europe, 2015).
2. Fuchs, R., Herold, M., Verburg, P. H., Clevers, J. G. P. W. & Eberle, J. Gross changes in reconstructions of historic land cover/use for Europe between 1900 and 2010. *Global Change Biol.* **21**, 299–313 (2015).

3. Ciais, P. et al. Carbon accumulation in European forests. *Nat. Geosci.* **1**, 425–429 (2008).
4. Senf, C. et al. Canopy mortality has doubled across Europe's temperate forests in the last three decades. *Nat. Commun.* **9**, 4978 (2018).
5. Seidl, R., Schelhaas, M.-J. & Lexer, M. J. Unraveling the drivers of intensifying forest disturbance regimes in Europe. *Global Change Biol.* **17**, 2842–2852 (2011).
6. Senf, C. & Seidl, R. Natural disturbances are spatially diverse but temporally synchronized across temperate forest landscapes in Europe. *Global Change Biol.* **24**, 1201–1211 (2018).
7. Senf, C., Sébald, J. & Seidl, R. Increases in canopy mortality and their impact on the demographic structure of Europe's forests. Preprint at *bioRxiv* <https://doi.org/10.1101/2020.03.30.015818> (2020).
8. Nabuurs, G.-J. et al. First signs of carbon sink saturation in European forest biomass. *Nat. Clim. Change* **3**, 792–796 (2013).
9. Seidl, R., Schelhaas, M. J., Rammer, W. & Verkerk, P. J. Increasing forest disturbances in Europe and their impact on carbon storage. *Nat. Clim. Change* **4**, 806–810 (2014).
10. Thom, D. & Seidl, R. Natural disturbance impacts on ecosystem services and biodiversity in temperate and boreal forests. *Biol. Rev.* **91**, 760–781 (2016).
11. Lindner, M. et al. Climate change impacts, adaptive capacity, and vulnerability of European forest ecosystems. *Forest Ecol. Manage.* **259**, 698–709 (2010).
12. Allen, C. D. et al. A global overview of drought and heat-induced tree mortality reveals emerging climate change risks for forests. *Forest Ecol. Manage.* **259**, 660–684 (2010).
13. Trumbore, S., Brando, P. & Hartmann, H. Forest health and global change. *Science* **349**, 814–818 (2015).
14. Millar, C. I., Stephenson, N. L. & Stephens, S. L. Climate change and forests of the future: managing in the face of uncertainty. *Ecol. Appl.* **17**, 2145–2151 (2007).
15. Seidl, R. The shape of ecosystem management to come: anticipating risks and fostering resilience. *BioScience* **64**, 1159–1169 (2014).
16. Turner, M. G. Disturbance and landscape dynamics in a changing world. *Ecology* **91**, 2833–2849 (2010).
17. Johnstone, J. F. et al. Changing disturbance regimes, ecological memory, and forest resilience. *Front. Ecol. Environ.* **14**, 369–378 (2016).
18. Bebi, P. et al. Changes of forest cover and disturbance regimes in the mountain forests of the Alps. *Forest Ecol. Manage.* **388**, 43–56 (2017).
19. Kulakowski, D., Bebi, P. & Rixen, C. The interacting effects of land use change, climate change and suppression of natural disturbances on landscape forest structure in the Swiss Alps. *Oikos* **120**, 216–225 (2011).
20. Munteanu, C. et al. Legacies of 19th century land use shape contemporary forest cover. *Glob. Environ. Change* **34**, 83–94 (2015).
21. Sommerfeld, A. et al. Patterns and drivers of recent disturbances across the temperate forest biome. *Nat. Commun.* **9**, 4355 (2018).
22. Lindenmayer, D. B. et al. Salvage harvesting policies after natural disturbance. *Science* **303**, 1303 (2004).
23. Senf, C., Müller, J. & Seidl, R. Post-disturbance recovery of forest cover and tree height differ with management in Central Europe. *Landsc. Ecol.* **34**, 2837–2850 (2019).
24. Thorn, S. et al. Impacts of salvage logging on biodiversity: a meta-analysis. *J. Appl. Ecol.* **55**, 279–289 (2018).
25. Janda, P. et al. The historical disturbance regime of mountain Norway spruce forests in the Western Carpathians and its influence on current forest structure and composition. *Forest Ecol. Manage.* **388**, 67–78 (2017).
26. Vacchiano, G., Garbarino, M., Lingua, E. & Motta, R. Forest dynamics and disturbance regimes in the Italian Apennines. *Forest Ecol. Manage.* **388**, 57–66 (2017).
27. Nagel, T. A. et al. The natural disturbance regime in forests of the Dinaric Mountains: a synthesis of evidence. *Forest Ecol. Manage.* **388**, 29–42 (2017).
28. Stephens, S. L. et al. Temperate and boreal forest mega-fires: characteristics and challenges. *Front. Ecol. Environ.* **12**, 115–122 (2014).
29. Brang, P. et al. Suitability of close-to-nature silviculture for adapting temperate European forests to climate change. *Forestry* **87**, 492–503 (2014).
30. Kulha, N. A. et al. At what scales and why does forest structure vary in naturally dynamic boreal forests? An analysis of forest landscapes on two continents. *Ecosystems* **22**, 709–724 (2019).
31. Duncker, P. S. et al. Classification of forest management approaches. *Ecol. Soc.* **17**, 51 (2012).
32. Levers, C. et al. Drivers of forest harvesting intensity patterns in Europe. *Forest Ecol. Manage.* **315**, 160–172 (2014).
33. Boncina, A. History, current status and future prospects of uneven-aged forest management in the Dinaric region: an overview. *Forestry* **84**, 467–478 (2011).
34. Kulakowski, D. et al. A walk on the wild side: disturbance dynamics and the conservation and management of European mountain forest ecosystems. *Forest Ecol. Manage.* **388**, 120–131 (2017).
35. Kuuluvainen, T., Tahvonen, O. & Aakala, T. Even-aged and uneven-aged forest management in boreal Fennoscandia: a review. *AMBIO* **41**, 720–737 (2012).
36. Kuemmerle, T., Hostert, P., Radloff, V. C., Perzanowski, K. & Kruhlav, I. Post-socialist forest disturbance in the Carpathian border region of Poland, Slovakia, and Ukraine. *Ecol. Appl.* **17**, 1279–1295 (2007).
37. Forzieri, G. et al. A spatially explicit database of wind disturbances in European forests over the period 2000–2018. *Earth Syst. Sci. Data* **12**, 257–276 (2020).
38. San-Miguel-Ayanz, J., Moreno, J. M. & Camia, A. Analysis of large fires in European Mediterranean landscapes: lessons learned and perspectives. *Forest Ecol. Manage.* **294**, 11–22 (2013).
39. Mori, A. S. & Kitagawa, R. Retention forestry as a major paradigm for safeguarding forest biodiversity in productive landscapes: a global meta-analysis. *Biol. Conserv.* **175**, 65–73 (2014).
40. Meigs, G. W. et al. More ways than one: mixed-severity disturbance regimes foster structural complexity via multiple developmental pathways. *Forest Ecol. Manage.* **406**, 410–426 (2017).
41. Hermosilla, T., Wulder, M. A., White, J. C., Coops, N. C. & Hobart, G. W. Regional detection, characterization, and attribution of annual forest change from 1984 to 2012 using Landsat-derived time-series metrics. *Remote Sens. Environ.* **170**, 121–132 (2015).
42. Olofsson, P. et al. Good practices for estimating area and assessing accuracy of land change. *Remote Sens. Environ.* **148**, 42–57 (2014).
43. Potapov, P. V. et al. Eastern Europe's forest cover dynamics from 1985 to 2012 quantified from the full Landsat archive. *Remote Sens. Environ.* **159**, 28–43 (2015).
44. Senf, C., Pflugmacher, D., Hostert, P. & Seidl, R. Using Landsat time series for characterizing forest disturbance dynamics in the coupled human and natural systems of Central Europe. *ISPRS J. Photogramm. Remote Sens.* **130**, 453–463 (2017).
45. Kennedy, R. E. et al. Spatial and temporal patterns of forest disturbance and regrowth within the area of the Northwest Forest Plan. *Remote Sens. Environ.* **122**, 117–133 (2012).
46. Hermosilla, T., Wulder, M. A., White, J. C., Coops, N. C. & Hobart, G. W. An integrated Landsat time series protocol for change detection and generation of annual gap-free surface reflectance composites. *Remote Sens. Environ.* **158**, 220–234 (2015).
47. Cohen, W. B., Yang, Z. & Kennedy, R. Detecting trends in forest disturbance and recovery using yearly Landsat time series: 2. TimeSync—tools for calibration and validation. *Remote Sens. Environ.* **114**, 2911–2924 (2010).
48. Pflugmacher, D., Rabe, A., Peters, M. & Hostert, P. Mapping pan-European land cover using Landsat spectral-temporal metrics and the European LUCAS survey. *Remote Sens. Environ.* **221**, 583–595 (2019).
49. Kennedy, R. E., Yang, Z. & Cohen, W. B. Detecting trends in forest disturbance and recovery using yearly Landsat time series: 1. LandTrendr—temporal segmentation algorithms. *Remote Sens. Environ.* **114**, 2897–2910 (2010).
50. Kennedy, R. et al. Implementation of the LandTrendr algorithm on Google Earth Engine. *Remote Sens.* **10**, 691 (2018).
51. Roy, D. P. et al. Characterization of Landsat-7 to Landsat-8 reflective wavelength and normalized difference vegetation index continuity. *Remote Sens. Environ.* **185**, 57–70 (2016).
52. Flood, N. Seasonal composite landsat TM/ETM+ images using the medoid (a multi-dimensional median). *Remote Sens.* **5**, 6481–6500 (2013).
53. Pflugmacher, D., Cohen, W. B. & E. Kennedy, R. Using Landsat-derived disturbance history (1972–2010) to predict current forest structure. *Remote Sens. Environ.* **122**, 146–165 (2012).
54. Cohen, W. B., Yang, Z., Healey, S. P., Kennedy, R. E. & Gorelick, N. A. LandTrendr multispectral ensemble for forest disturbance detection. *Remote Sens. Environ.* **205**, 131–140 (2018).
55. Senf, C., Pflugmacher, D., Wulder, M. A. & Hostert, P. Characterizing spectral-temporal patterns of defoliator and bark beetle disturbances using Landsat time series. *Remote Sens. Environ.* **170**, 166–177 (2015).
56. Breiman, L. Random forests. *Mach. Learn.* **45**, 5–32 (2001).
57. Cohen, W. et al. How similar are forest disturbance maps derived from different landsat time series algorithms? *Forests* **8**, 98 (2017).
58. Birch, C. P. D., Oom, S. P. & Beecham, J. A. Rectangular and hexagonal grids used for observation, experiment and simulation in ecology. *Ecol. Model.* **206**, 347–359 (2007).
59. Bright, B. C., Hudak, A. T., Kennedy, R. E. & Meddens, A. J. H. Landsat time series and Lidar as predictors of live and dead basal area across five bark beetle-affected forests. *IEEE J. Sel. Top. Appl. Earth Obs. Remote Sens.* **7**, 3440–3452 (2014).
60. Wilcox, R. R. *Fundamentals of Modern Statistical Methods: Substantially Improving Power and Accuracy* (Springer, 2010).

Acknowledgements

C.S. acknowledges funding from the Austrian Science Fund (FWF) Lise Meitner Programme (no. M2652). R.S. acknowledges funding from FWF START

grant no. Y895-B25. We thank J. Braaten (Oregon State University) for making the code of LandTrendr open source, which greatly helped in implementation of this research.

Author contributions

C.S. and R.S. designed the research. C.S. performed all computations and analyses. C.S. wrote the manuscript with input from R.S.

Competing interests

The authors declare no competing interests.

Additional information

Extended data is available for this paper at <https://doi.org/10.1038/s41893-020-00609-y>.

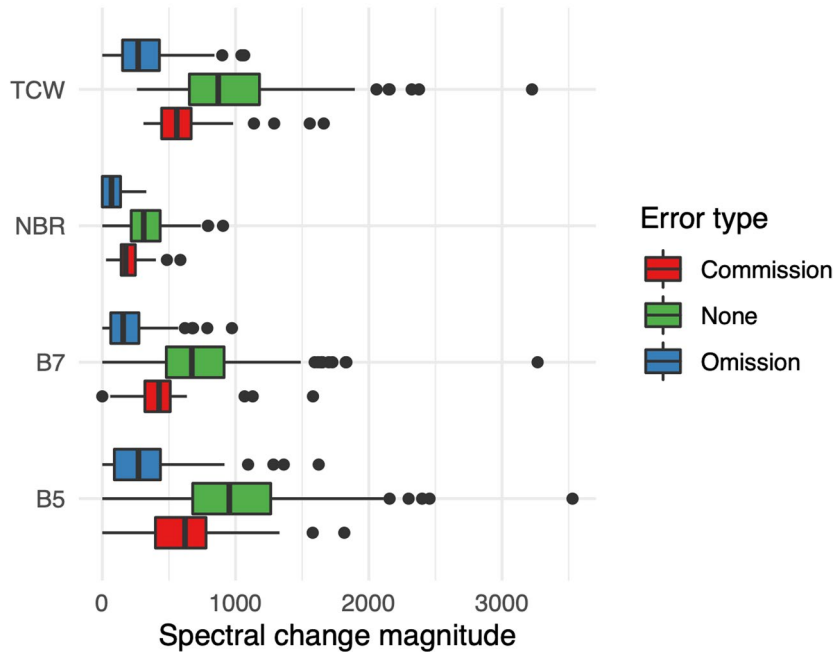
Supplementary information is available for this paper at <https://doi.org/10.1038/s41893-020-00609-y>.

Correspondence and requests for materials should be addressed to C.S.

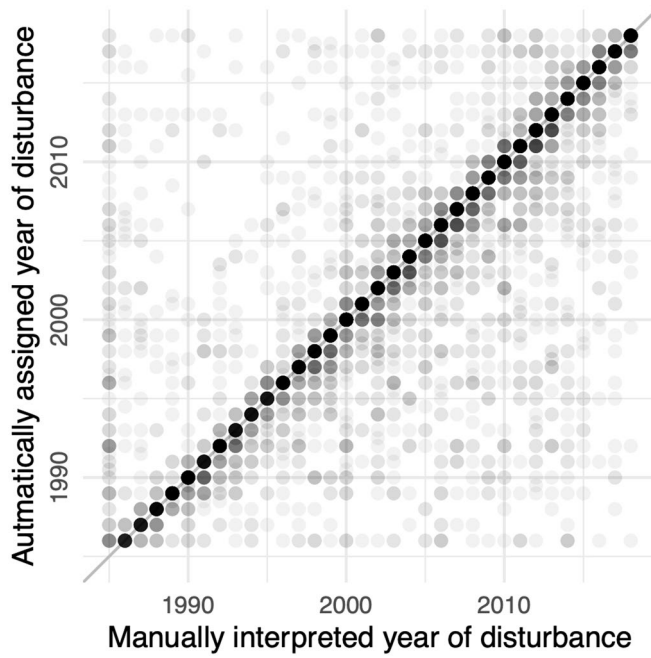
Reprints and permissions information is available at www.nature.com/reprints.

Publisher's note Springer Nature remains neutral with regard to jurisdictional claims in published maps and institutional affiliations.

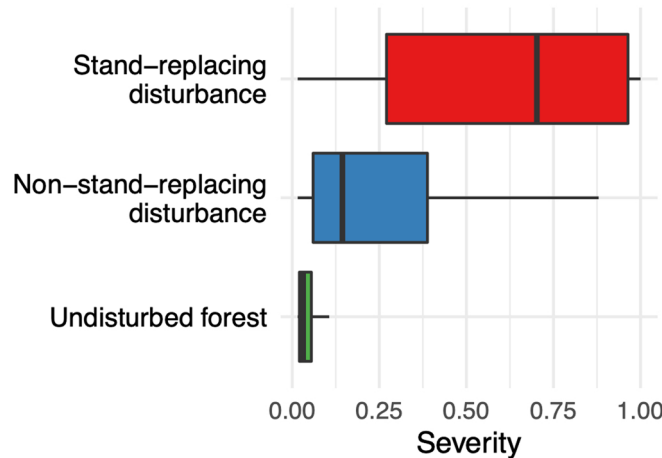
© The Author(s), under exclusive licence to Springer Nature Limited 2020, corrected publication 2021



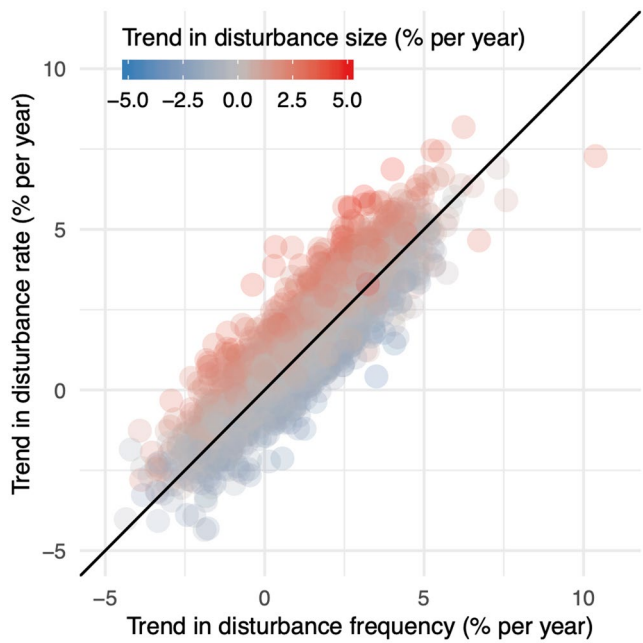
Extended Data Fig. 1 | Analysis of map omission and commission errors. Spectral change magnitude in Tasseled Cap Wetness (TCW), Normalized Burn Ration (NBR), Landsat shortwave-infrared I (B5), and Landsat shortwave-infrared II (B7) for all validation pixels ($n = 5,000$) with commission errors, omission errors and no error (i.e., matching label between mapped and interpreted). For omission errors, spectral change magnitudes were substantially lower than for correctly classified disturbances, highlighting that many omission errors stem from very low spectral changes, indistinguishable from noise in currently available Landsat-based time series methods.



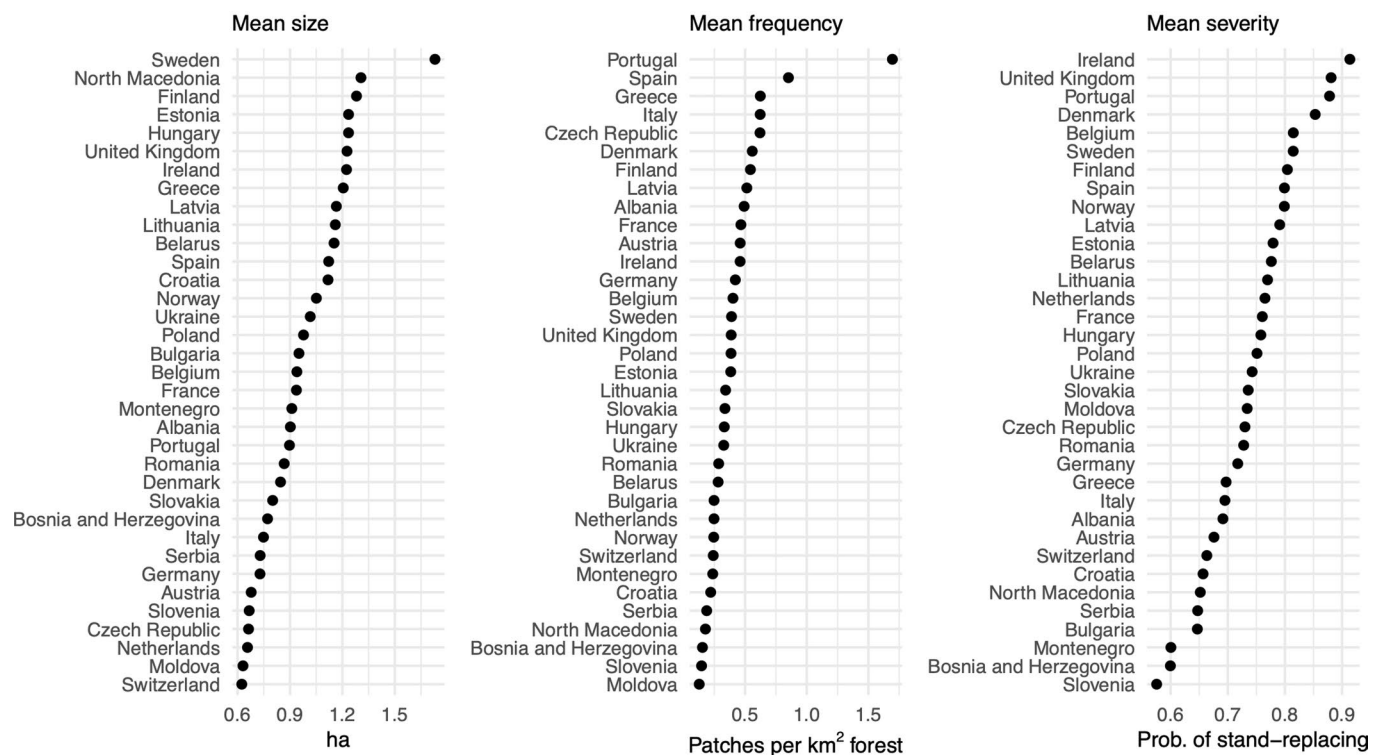
Extended Data Fig. 2 | Validation of the disturbance year. Estimated disturbance year versus manually interpreted year of disturbance for 5,000 independent reference pixels. The majority of the pixels is on or close to the 1:1-line, indicating that the correct year of disturbance was assigned. The hue indicates data point density (higher hue = more data points).



Extended Data Fig. 3 | Validation of disturbance severity. Distribution of estimated disturbance severities (i.e., the probability that a pixel has lost its complete canopy during disturbance) among pixels classified as stand-replacing disturbances, non-stand-replacing disturbances and undisturbed forest. The classification labels were derived from reference data and are based on a manual interpretation of Landsat time series and auxiliary use of aerial photos. Stand-replacing disturbances have the highest disturbance severities and are well separated from non-stand-replacing disturbances.

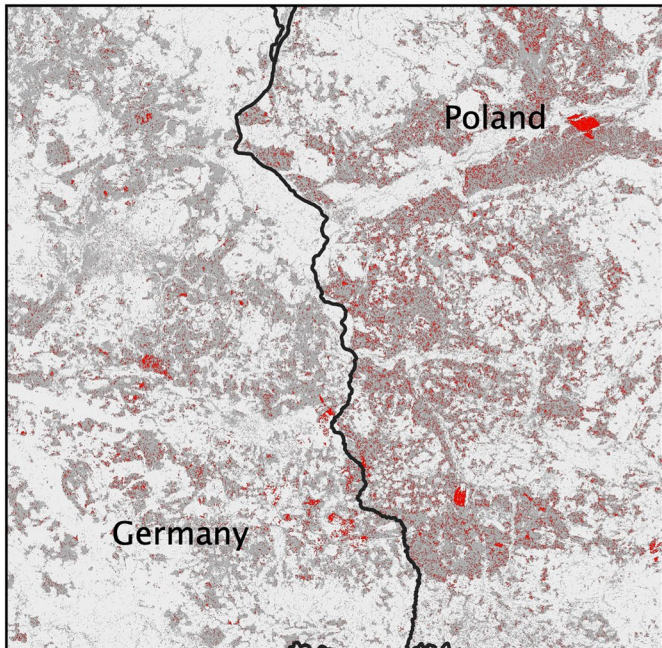


Extended Data Fig. 4 | Relationship between changing disturbance rates, disturbance frequencies, and disturbance sizes. Changes in disturbance rates (y-axis; percent of forest area disturbed) in relation to changes in disturbance size (color) and disturbance frequency (x-axis). Trends in disturbance rates are mainly explained by changes in disturbance frequencies (71 %), while changes in disturbance size explained a substantial lower proportion of the variability (24 %).

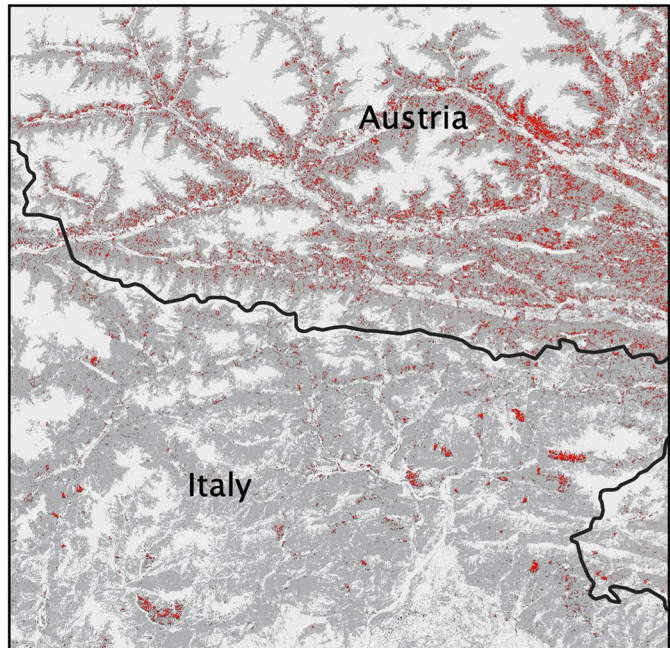


Extended Data Fig. 5 | Country-wise disturbance regime indicators. Mean disturbance size, frequency and severity summarized for each country of this study. For exact values and other country-wise statistics, please see Supplementary Table 3.

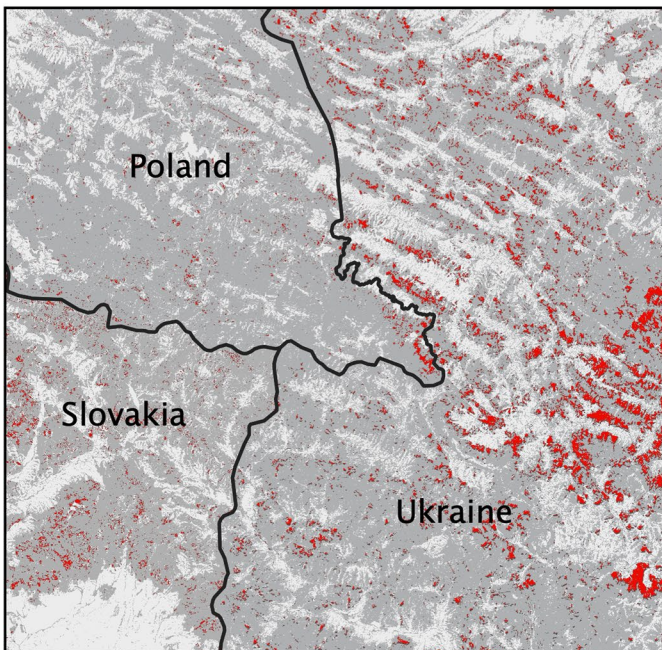
Central European Mixed Forests



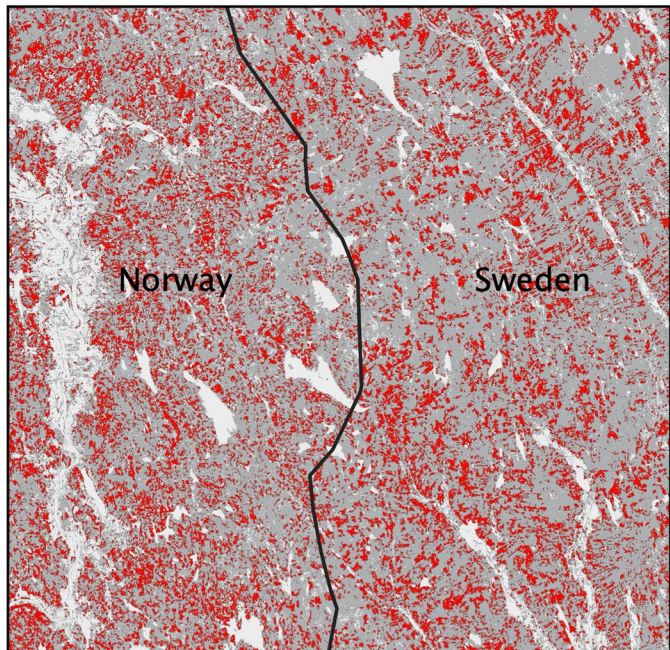
Alps Conifer and Mixed Forests



Carpathian Montane Forests

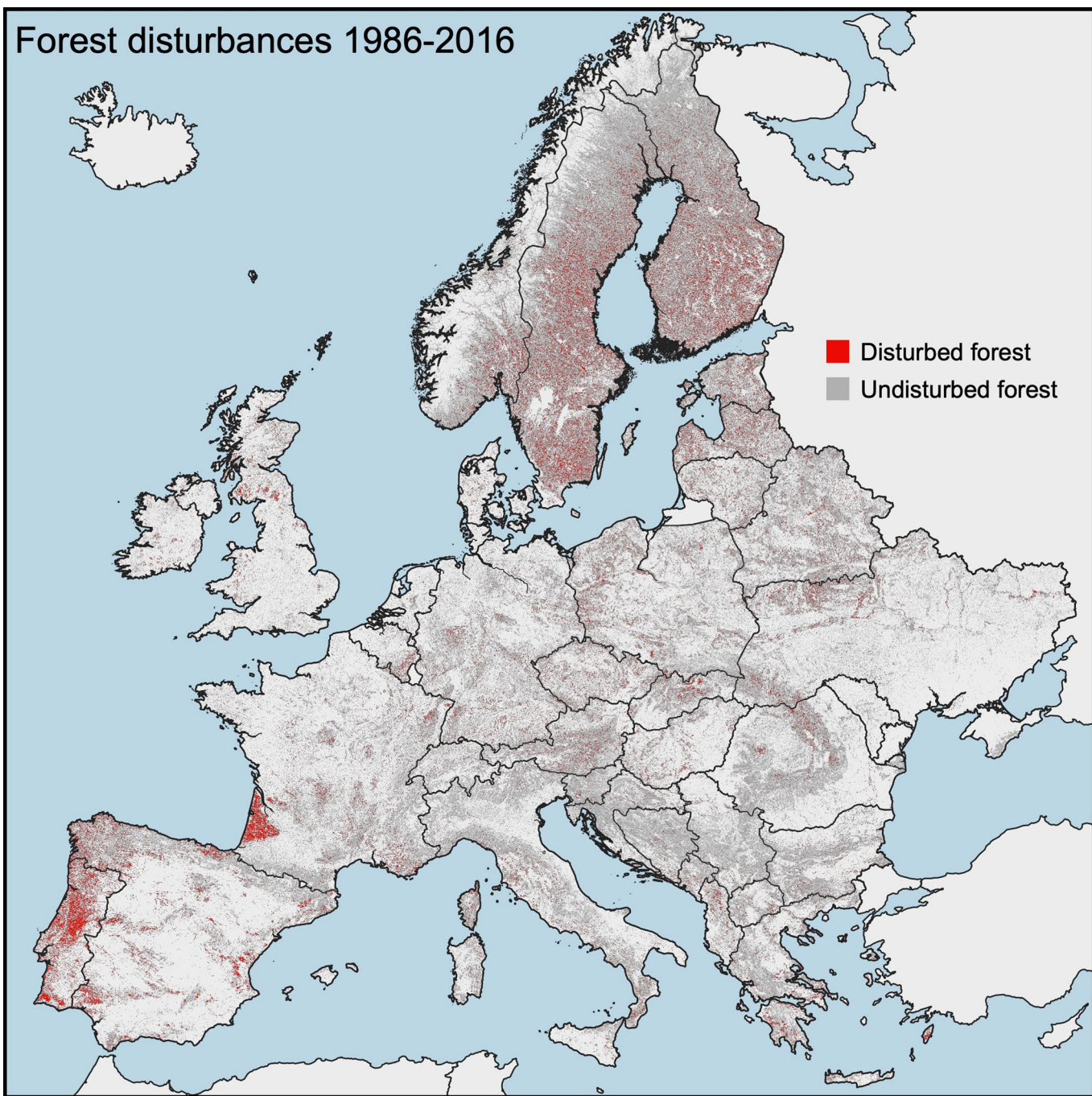


Scandinavian and Russian Taiga



Extended Data Fig. 6 | Examples of differences in disturbance regimes among countries with varying forest management. Differences in spatial disturbance patterns between countries in similar ecoregions and with similar forest types: (1) Central European Mixed Forests with larger and more frequent disturbances in Poland compared to Germany. (2) Alps Conifer and Mixed Forests with substantially higher disturbance frequencies in Austria compared to Italy. (3) Carpathian Montane Forests, with widely varying disturbance sizes and frequencies between Poland, Slovakia and Ukraine. (4) Scandinavian and Russian Taiga with differences in disturbance size between Norway and Sweden. Background maps are from <https://gadm.org>.

Forest disturbances 1986-2016



Extended Data Fig. 7 | Forest disturbances in Europe 1986-2016. Large version of the disturbance map shown in Fig. 1a for presentation. Background maps are from <https://gadm.org>.

Reporting Summary

Nature Research wishes to improve the reproducibility of the work that we publish. This form provides structure for consistency and transparency in reporting. For further information on Nature Research policies, see our [Editorial Policies](#) and the [Editorial Policy Checklist](#).

Statistics

For all statistical analyses, confirm that the following items are present in the figure legend, table legend, main text, or Methods section.

n/a Confirmed

- The exact sample size (n) for each experimental group/condition, given as a discrete number and unit of measurement
- A statement on whether measurements were taken from distinct samples or whether the same sample was measured repeatedly
- The statistical test(s) used AND whether they are one- or two-sided
Only common tests should be described solely by name; describe more complex techniques in the Methods section.
- A description of all covariates tested
- A description of any assumptions or corrections, such as tests of normality and adjustment for multiple comparisons
- A full description of the statistical parameters including central tendency (e.g. means) or other basic estimates (e.g. regression coefficient) AND variation (e.g. standard deviation) or associated estimates of uncertainty (e.g. confidence intervals)
- For null hypothesis testing, the test statistic (e.g. F , t , r) with confidence intervals, effect sizes, degrees of freedom and P value noted
Give P values as exact values whenever suitable.
- For Bayesian analysis, information on the choice of priors and Markov chain Monte Carlo settings
- For hierarchical and complex designs, identification of the appropriate level for tests and full reporting of outcomes
- Estimates of effect sizes (e.g. Cohen's d , Pearson's r), indicating how they were calculated

Our web collection on [statistics for biologists](#) contains articles on many of the points above.

Software and code

Policy information about [availability of computer code](#)

Data collection No primary data was collected in this study. Satellite data was provided by the United States Geological Survey (USGS) Landsat archive.

Data analysis Satellite data was processed using peer-reviewed code available through the cloud-computing platform Google Earth Engine. Summary statistics were created in R, Version 4.0.2.

For manuscripts utilizing custom algorithms or software that are central to the research but not yet described in published literature, software must be made available to editors and reviewers. We strongly encourage code deposition in a community repository (e.g. GitHub). See the Nature Research [guidelines for submitting code & software](#) for further information.

Data

Policy information about [availability of data](#)

All manuscripts must include a [data availability statement](#). This statement should provide the following information, where applicable:

- Accession codes, unique identifiers, or web links for publicly available datasets
- A list of figures that have associated raw data
- A description of any restrictions on data availability

The Landsat data is freely available via the USGS Earth Explorer (<https://earthexplorer.usgs.gov>) or via the Google Earth Engine (<https://earthengine.google.com>). The reference data used herein is available under: <https://doi.org/10.5281/zenodo.3561925>. All other data are available under: <https://doi.org/10.5281/zenodo.3925447>. The disturbance maps produced in this paper are available under: <https://doi.org/10.5281/zenodo.3924381>.

Field-specific reporting

Please select the one below that is the best fit for your research. If you are not sure, read the appropriate sections before making your selection.

Life sciences Behavioural & social sciences Ecological, evolutionary & environmental sciences

For a reference copy of the document with all sections, see nature.com/documents/nr-reporting-summary-flat.pdf

Ecological, evolutionary & environmental sciences study design

All studies must disclose on these points even when the disclosure is negative.

Study description	We mapped forest disturbance from satellite data continuously across Europe and summarized spatial patterns and temporal trends at a regular grid.
Research sample	There is no sampling, as we have continuous coverage data (i.e., maps).
Sampling strategy	N/A
Data collection	Satellite data was obtained from the USGS Landsat archive.
Timing and spatial scale	The data covers the time period 1984-2018, which is the full time coverage of the Landsat archive. However, no disturbances were mapped for the years 1984-1985 and 2017-2018, as disturbance detection in the beginning and end of the time series is impossible with current methods. The spatial extent is continental Europe.
Data exclusions	No data was excluded, but due to methodological restriction of current methods, no disturbance maps for the year 1984-1985 and 2017-2018 could be created. Spatially, we excluded countries smaller 10,000 km ² (Lichtenstein, Luxembourg, Monte Carlo and Malta), as well as the Russian oblast of Kalingrad.
Reproducibility	The full data processing can be reproduced and has been reproduced several times.
Randomization	N/A
Blinding	N/A

Did the study involve field work? Yes No

Reporting for specific materials, systems and methods

We require information from authors about some types of materials, experimental systems and methods used in many studies. Here, indicate whether each material, system or method listed is relevant to your study. If you are not sure if a list item applies to your research, read the appropriate section before selecting a response.

Materials & experimental systems

- | | |
|-------------------------------------|--|
| n/a | Involved in the study |
| <input checked="" type="checkbox"/> | <input type="checkbox"/> Antibodies |
| <input checked="" type="checkbox"/> | <input type="checkbox"/> Eukaryotic cell lines |
| <input checked="" type="checkbox"/> | <input type="checkbox"/> Palaeontology and archaeology |
| <input checked="" type="checkbox"/> | <input type="checkbox"/> Animals and other organisms |
| <input checked="" type="checkbox"/> | <input type="checkbox"/> Human research participants |
| <input checked="" type="checkbox"/> | <input type="checkbox"/> Clinical data |
| <input checked="" type="checkbox"/> | <input type="checkbox"/> Dual use research of concern |

Methods

- | | |
|-------------------------------------|---|
| n/a | Involved in the study |
| <input checked="" type="checkbox"/> | <input type="checkbox"/> ChIP-seq |
| <input checked="" type="checkbox"/> | <input type="checkbox"/> Flow cytometry |
| <input checked="" type="checkbox"/> | <input type="checkbox"/> MRI-based neuroimaging |